Magnesium Technology 2014
Edited by: Martyn Alderman, Michele V. Manuel, Norbert Hort, and Neale R. Neelameggham
TMS (The Minerals, Metals & Materials Society), 2014

EMERGING APPLICATIONS USING MAGNESIUM ALLOY POWDERS: A FEASIBILITY STUDY

Rajiv Tandon and Deepak Madan
Magnesium Elektron Powders, 2590 Ridgeway Blvd, Manchester NJ 08759, USA

Keywords: magnesium powders, lightweight, powder metallurgy

Abstract

The use of powder metallurgy offers a potential processing route based on tailored compositions and unique microstructures to achieve high performance in magnesium alloys. This paper highlights recent advances in the production, qualification, and characterization of gas atomized AZ91E, WE43 and Elektron21 alloy powders. Transmission electron microscopy (TEM) was used to understand the bulk and surface structure of the atomized powder. The potential for using these magnesium alloy powders for emerging applications involves establishing compatibility with viable consolidation processes such as cold spray, laser assisted deposition, forging and extrusion. This study summarizes the preliminary results for various ongoing investigations using WE43 powder as an example. Results show that powder metallurgy processed WE43 results in comparable properties to those obtained from cast and wrought and offers potential for improvement.

Introduction

Background

There is an emerging interest in the use of magnesium alloys in various engineering applications which are driven largely by the need for lightweighting to achieve higher levels of fuel efficiency [1-6]. Several powder metallurgy routes are being investigated with the goal of targeting novel compositions and unique microstructures leading to high performance lightweight magnesium applications. Rapidly solidified powder and the use of nanostructured powder have been studied and reported in the literature with promising results [7-10]. For example, tensile yield strengths of 610 MPa (87 ksi) with an elongation of 5% have been reported for a Mg-0.8Zn-2.1Y alloy [7], and yield strength of 425 MPa (60 ksi) with an elongation of 9.6% have been reported for a Mg-6Al-0.5Mn-2Ca alloy [8] using a powder metallurgy approach.

Other magnesium powder based manufacturing processes in the early stages of investigation include additive manufacturing [11], metal injection molding [12,13], and cold spray. Additive manufacturing and metal injection molding offer a unique path for fabricating intricate components, such as Mg alloy based bio-absorbable implants. Cold spray technology using Mg alloy powders offers a potentially novel approach to repair and refurbish expensive Mg castings and structures that have to be taken out of service due to wear and corrosion, in addition to fabricating near net shaped structures such as casings and liners.

Most of the published work in the literature has relied on laboratory scale powder manufacturing and consolidation methods. To some extent, these approaches have been based on alleviating concerns about magnesium powder production and handling. To develop a commercial scale process it is important to establish at the onset the compatibility of Mg alloy powders with the processing hardware and equipment, while taking into account the specific characteristics of that particular magnesium alloy.

Recently, a scalable technology for the production of atomized magnesium alloy powders was established based on collaboration between the US Army Research Laboratory (ARL), US Army RDECOM and Magnesium Elektron Powders. Gas atomized AZ91E, WE43, and Elektron21 powders have been developed and characterized. In a parallel effort, prealloyed powders having the same composition as the above mentioned alloys were also produced on a commercial scale by grinding. Selected consolidation routes including forging, extrusion, cold spray deposition, and laser additive deposition were investigated using the WE43 prealloyed powder and early stage results are discussed in this paper.

Procedure

Magnesium Alloy Powders: Magnesium alloy powders AZ91E, WE43, and Elektron21 were produced using an inert gas atomization process. Figure 1 shows the cross section optical micrographs of the lightly etched -100/+325 mesh fractions for the three atomized powders. All three powders showed a fine dendritic microstructure resulting from the rapid solidification during the atomization process. The interdendritic spacing for all three alloys were measured between 1 to 3 microns for the -100/+325 mesh distribution.

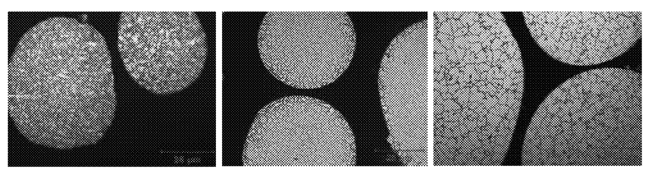

(a) (b) (c)

Figure 1. Optical micrographs of (a) gas atomized AZ91E -100/+325 mesh, (b) gas atomized WE43 -100/+325 mesh and (c) gas atomized Elektron21 -100/+325 mesh, alloy powders.

The powder characteristics of the three atomized magnesium alloy powders are shown in Table I. The -325 mesh fraction was non free flowing. All three powders had similar tap density and flow rate behavior for similar size fractions.

The atomized WE43 alloy powder was prepared via FIB-INLO technique for TEM analysis. Figure 2 shows two adjacent powder particles mounted in epoxy. The surface and bulk region of one of the particles (shown by inset photo of Powder 2) was analyzed using X-ray Energy Dispersive Spectrometry (XEDS). The surface region of the powder in area 1 shows the presence of oxygen and rare earth elements such as Nd and Y, as compared to the bulk region in area 2. Enrichment of Y, Nd, Gd, and Sm was also observed in the interdendritic regions of the solidified powder. The presence of surface oxygen can be attributed to a passive film that is created during the atomization process.

Table I. Apparent density, tap density, flow rate, and particle size distribution for atomized magnesium alloy powders.

Powder Designation	Apparent Density g/cm^3	Tap Density g/cm^3	Flow Rate s/50g	D_{10}, D_{50}, D_{90} µm
AZ91E -325 mesh	0.75	0.93	No flow	7, 21, 41
AZ91E -100/+325 mesh	0.97	1.09	73	55, 94, 153
WE-43 -325 mesh	0.78	0.94	No flow	7, 21, 40
WE-43 -100/+325 mesh	0.99	1.09	67	50, 83, 133
E-21 -325 mesh	0.75	0.89	No flow	7, 21, 42
E-21 -100/+325 mesh	1.0	1.11	79	50, 95, 163

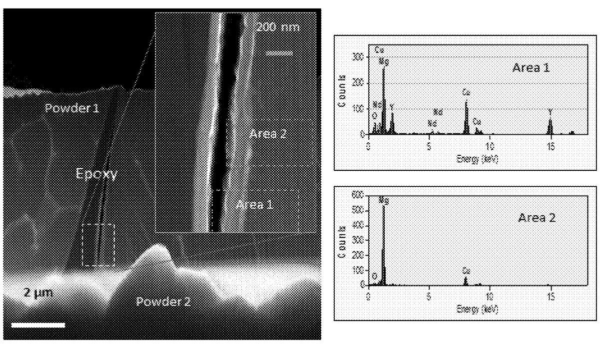

Figure 2. TEM image of the cross section of atomized WE43 powder showing the surface and interior regions of powder and the elemental segregation.

Forging: Atomized WE43 powder (80/325 mesh) with a d_{50} of 90µm was used for powder forging. The powder was first consolidated into a preform using cold isostatic pressing and subsequently forged by heating and placing in a granular pressure transmitting media. One billet was subsequently forged a second time (double forged). The single forged billet was approximately 10 cm in diameter and 13 cm in height, wand weighed 2.5kg. The double forged billet was approximately 12 cm in diameter and 11.4 cm in diameter. The billet was machined into tensile specimens of 0.64 cm gauge diameter and 2.54 cm gauge length and tested according to ASTM E8-09 as shown in Figure 3.

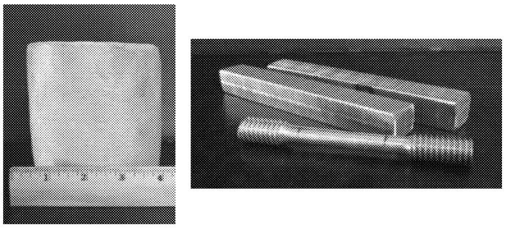

Figure 3. Tensile specimens machined from the forged billet.

Rolling: A feasibility study into rolling was also performed on the consolidated WE43 billet. For the rolling trials a forged cylinder was machined into flat plates by water-jet cutting into 0.64 cm thick sections. The plates were preheated between 340-470°C and rolled at 10, 15 and 20% reduction per pass for total reduction ranging from 50 to 72%, as shown in Figure 4.

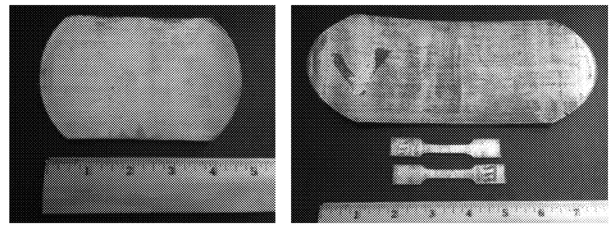

(a) (b)

Figure 4. Photographs showing (a) a 0.64cm thick plate used for rolling trials, and (b) a rolled plate and the tensile specimens machined from a rolled plate.

The forged WE43 generally exhibited good formability under the rolling conditions used. However, it was noted that a 20% reduction per pass resulted in cracks and tears along the edges and in transverse direction. Some of these defects resulted from pre-existing surface flaws. Mechanical properties were measured on two rolled plates that were rolled at 10% reduction per pass for a total of 72% reduction in thickness.

Laser Deposition: Laser deposition trials using atomized WE43 were conducted using a customized setup which involved fabrication of an inert gas purged glove box with an oxygen sensor. This was done to address potential flammability concerns. The laser head and the powder feed nozzle were placed inside the glove box and a preplaced powder bed of varying thickness was used to initially conduct trials by changing laser power (from 500 to 1000W), travel speed (12.7 to 50.8 cm/min), and powder depth (from 0.254 to 0.508 mm). A total of 48 trials were run and samples were examined macroscopically for voids, quality of deposit and cross sectioned to examine internal microstructure. Further trials were performed to study multipass builds. After narrowing the process window, multi pass builds were conducted using a coaxial powder feed nozzle on a WE43 wrought substrate (that had been heat treated to a T5 condition [15]). For these deposits, the Vickers microhardness was measured to determine hardness profile across the interface.

Cold Spray Deposition: Feasibility studies were performed using a CGT Kinetics 400 High Pressure Cold Spray System. Both the -400 mesh ground powder (AZ31B) and gas atomized powder (WE43) were evaluated. Process parameters that were investigated included the gas pressure, gas temperature, gas flow, powder flow and stand-off distance. A polymer DeLaval spray nozzle was used and helium was used as a process gas. The coatings were examined optically for microstructure. Hardness and density (using image analysis) were also measured.

Results and Discussions

The optical micrographs of the gas atomized WE43 (single and double forged) powder billet are shown in Figure 5. The gas atomized WE43 powder resulted in a homogeneous microstructure with well dispersed precipitates in the matrix, along with the presence of prior particle grain boundaries. There were no significant differences between the microstructures of the single and double forged atomized WE43.

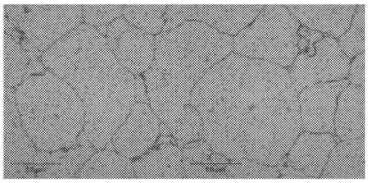

(a) (b)

Figure 5. Optical micrographs of (a) single forged gas atomized WE43 and (c) double forged atomized WE43.

The microstructure of the rolled WE43 plate along the rolling direction and the short transverse direction is shown in Figures 6a and 6b, respectively. This plate was rolled at 10% reduction per pass to a 72% total reduction. The grain elongation is evident in the micrographs. The resulting anisotropy was not studied in this investigation.

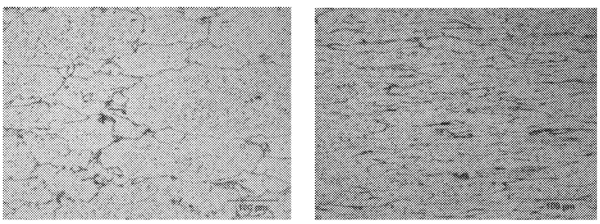

(a) (b)

Figure 6. Optical micrographs of WE43 along (a) longitudinal rolling direction, and (b) short transverse direction, showing grain elongation.

The mechanical properties of the ground and gas atomized WE43 powders consolidated using forging and rolling are compared in Figure 7. Also shown are typical values of WE43B alloy produced via extrusion, forging and casting (each in a heat treated T6 condition). The prefix SF and DF refer to single forged and double forged condition, while Long. and Trans. refer to longitudinal and transverse direction, respectively.

The graph highlights several important results. For example, the main difference between the ground WE43 and gas atomized WE43 powder was manifested mainly in terms of an enhanced ductility for the atomized powder as seen in the results of single-forged specimen in the longitudinal direction. The yield strength and UTS for the ground WE43 and atomized WE43 were quite similar (at approximately 200 and 245 MPa, respectively), while there was a significant improvement in overall ductility from 3.5 to 6.5%. This is attributed to a more homogenous microstructure and a significantly thinner surface passive film on the surface of the atomized powder as compared to the ground powder.

A similar trend was observed on comparing the single-forged and double-forged atomized WE43. The yield strength and UTS were similar except for a gain in ductility of almost 50%. The reasons for the differences in ductility are under investigation.

On comparing the atomized single and double-forged WE43 to the rolled WE43 in both the longitudinal and transverse directions, it can be seen that there was a significant increase to the yield strength (from approximately 200MPa to 280MPa) and UTS (from approximately 250MPa to 300MPa) by rolling. The rolled WE43 exhibited a ductility of about 6% even after significant work hardening.

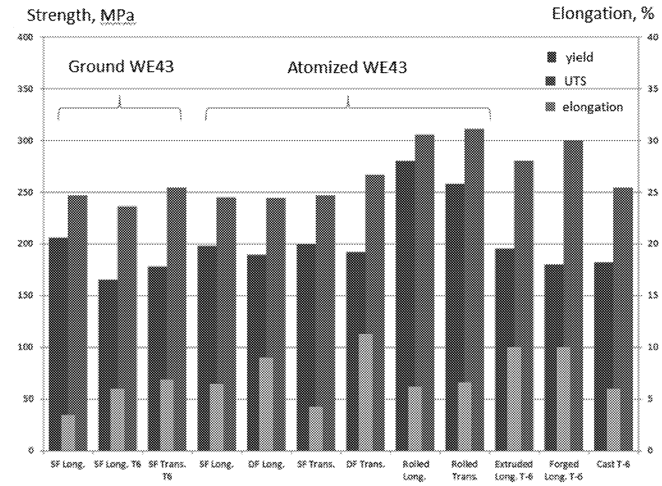

Figure 7. Typical mechanical properties of the P/M consolidated ground and atomized WE43 alloy comparison against commercial extruded, forged, and cast WE43B [14,15].

Laser deposition studies showed that an increase in laser power had a positive impact on the overall quality of the deposits as shown in Figure 8. The samples shown were tested with a bed height of 0.5mm and using a speed of 50cm/min. The top surfaces of multi-pass and multi-layer builds appeared acceptable, with no obvious macroscopic defects.

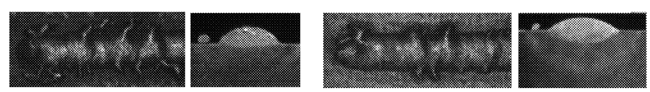

870 W 1000W

Figure 8. Top surface and cross sections of samples deposited at 870W and 1000W.

However, cross sections of the pre-placed powder bed deposits showed the presence of pores on the top portion of the weld bead. The circular shape of the pores was indicative of gaseous desorption which can be observed in the WE43 alloy. An example cross section of gas pores is shown in Figure 9(a) which was deposited at 870W and 38mm/min. These pores can be mitigated with improvements to the processing parameters. Figure 9(b) shows the grain coarsening associated with the heat affected zone.

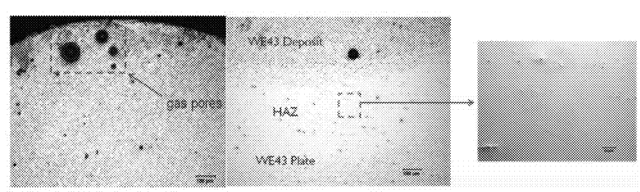

a b

Figure 9. Cross section showing (a) gas pores on top surface of the deposit, and (b) grain coarsening in the HAZ of sample deposited at 870W at 38mm/min.

By comparison, using a commercial co-axial powder feeder for multipass and multilayer deposits resulted in improved results and showed significantly lower levels of porosity as compared to the preplaced powder approach.

The microhardness plot of the sample deposited at 1750W is shown in Figure 10. The graph shows a hardness drop across the heat affected zone (HAZ) into the deposited layer. The hardness of the base metal was measured to be about 104 HVN using a 300g load. There was no statistical difference in the hardness values between the HAZ and the deposited layer (both had mean values of 74VHN). Further metallurgical investigations and heat treatment studies are being performed to fully characterize the HAZ and the deposited layer.

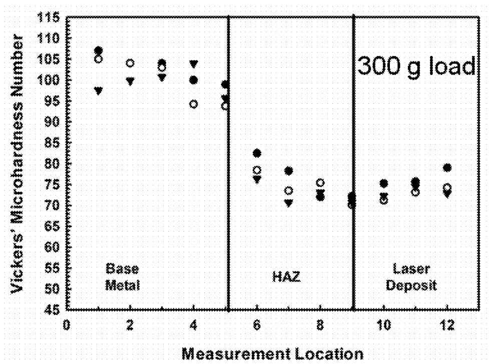

Figure 10. Hardness profile across the three layer buildup, five pass wide sample made using co-axial powder feeder at 1750W (speed: 63.5 cm/min).

The results of cold spray tests showed that it was possible to use both ground powder and atomized powder and obtain high density coatings. The result using ground AZ31B powder is shown in Figure 11. The optical micrographs show that by increasing the gas temperature, there was an increase in the coating density. The peak hardness was obtained at about 300°C, above which the hardness decreased.

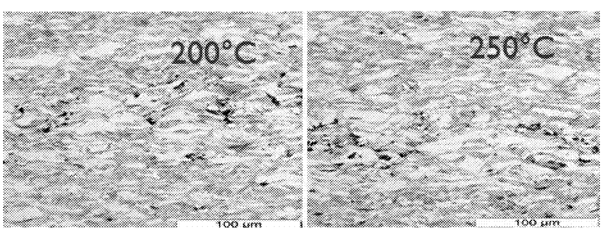

5.4% porosity, 146 HVN 3.7% porosity, 159 HVN

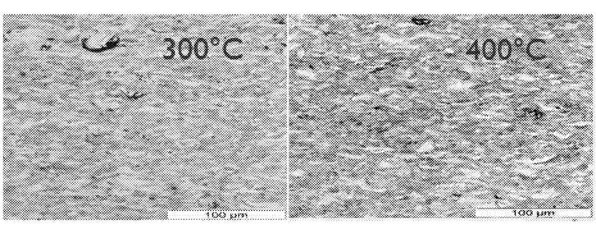

2.7% porosity, 161 HVN 2.5% porosity, 135 HVN

Figure 11. Effect of gas temperature on the porosity and hardness of -400 mesh AZ31B ground powder.

Improved results were obtained using gas atomized WE43 powder. Figure 12 shows effects of increasing gas pressure at 300°C on the cold sprayed coating microstructure. The deposited hardness and density increased by increasing the gas pressure from 25 bar to 34 bar.

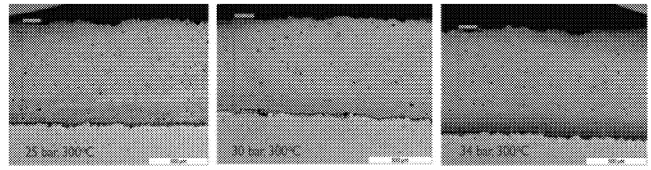

1% porosity 122 HVN 1.2% porosity 148 HVN 0.6% porosity 157 HVN

Figure 12. Effect of gas pressure on the cold spray microstructure of a gas atomized WE43 powder.

The deposition efficiency using cold spray was about 40%, which was below what experimental model had predicted. However, initial results are encouraging enough and warrant further optimization and characterization of resulting mechanical properties to determine suitability in their intended end applications.

Summary and Conclusions

The results of this study have shown that it is possible to obtain properties using commercially developed gas atomized WE43 alloy that match and, in some cases, exceed typical properties of extruded, forged and cast WE43B. Gas atomized Mg alloy powders with homogeneous fine scale microstructure and lower surface oxygen content lead to enhanced ductility as compared to mechanically ground powder. Further optimization work is planned to develop a more comprehensive understanding of structure-property relationship to justify the economics of a powder based approach. Investigating optimal heat treatment parameters, studying the effects of thermal processing history, and the influence of high shear rate deformation processes, such as extrusion, are ongoing.

It has also been demonstrated that Magnesium alloy powders can be cold sprayed using existing commercial powder coating system. The achievement of high density and high hardness is the first step towards optimization and conducting tests that are necessary to demonstrate their use in repair applications.

Investigations into laser deposition process using Mg based prealloyed powder such as WE43 have shown that under the right combination of laser powder and travel speed it is possible to obtain deposits that are visually acceptable using qualitative visual standards based on other alloy systems. However, the source of gas pores and its effect on deposited mechanical properties of the coating needs to be studied in the next step.

Acknowledgement

The authors would like to thank Dr. Yongho Sohn at the University of Central Florida for TEM analyses and Todd Palmer at Applied Research Lab, Penn State University for laser deposition investigation. Powder development was sponsored by the U.S. Army Research Laboratory and the U.S. Army Research, Development, and Engineering Center and was accomplished under Cooperative Agreement W911NF-10-2-002 and Army Contract W15QKN-09-C-2008.

References

1. R. Tandon *et.al*., "Magnesium Powder technology for Ultra Lightweight Applications," *Proceedings of The 2011 International Conference on Powder Metallurgy and Particulate Materials*, II (2011), Metal Powder Industries Federation, 07-157-07-163.

2. S. Mathaudhu, "Magnesium Alloys in U.S. Military Applications: Past, Current and Future Solutions", *Magnesium Technology 2010,* The Minerals, Metals and Materials Society, (2010) 27-32.

3. B. Gywnne, "Magnesium Alloys in Aerospace Applications-Flammability Testing and Results", *Magnesium Technology 2010*, The Minerals, Metals and Materials Society, (2010), 13.

4. K.Cho *et.al*, "Magnesium Technology and Manufacturing for Ultra Lightweight Armored Ground Vehicles", *Proceedings of the 2008 Army Science Conference,* Orlando, FL 2008.

5. Rick Delrome *et.al*., "Ultra Light Metallic Armor (ULMA)-Magnesium Hard Alloys as the Defense Against Modern Warfare Threats", *presented at Magnesium Technology 2010*, TMS 2010.

6. T. Jones, K. Kondoh, "Ballistic Analysis of New Military Grade Magnesium Alloys for Armor Applications", *Magnesium Technology 2011*, The Minerals, Metals and Materials Society, (2011) 425-430.

7. Y. Kawamura and A. Inoue, "Rapidly Solidified Powder Metallurgy Mg97Zn1Y2 Alloys with Tensile Yield Strength of 610 MPa and Elongation of *5%", Magnesium Technology 2002*, TMS (The Minerals, Metals and Materials Society), 2002.

8. A. Elsayed, J. Umeda, and K. Kondoh, "The Production of Powder Metallurgy Hot Extruded Mg-Al-Mn-Ca Alloy With High Strength and Limited Anisotropy", *Magnesium Technology 2011*, The Minerals, Metals and Materials Society, (2011) 475-480.

9. C.J. Bettles, M.H. Moss, and R. Lapovok, "A Mg-Al-Nd Alloy Produced via a Powder Metallurgical Route", *Materials Science and Engineering* A 515, (2009) 26-32.

10. V.M. Segal, "Engineering and Commercialization of Equal Channel Angular Extrusion (ECAE)", Materials Science and Engineering A 386, 2004, pp 269-276.

11. C.C. Ng *et. al*.,"Layer Manufacturing of Magnesium and its Alloy Structures for Future Applications," *Virtual and Physical Prototyping*, Vol 5, No.1, (2010), 13-19.

12. M. Wolff *et.al*.,"Properties of Sintered Mg Alloys for Biomedical Applications," *Materials Science Forum,* Vol.690, (2011) 491-494.

13. M. Wolff *et.al*.,"Advances in the Metal Injection Molding of Mg-Ca Alloys for Biomedical Applications," *PIM International,* Vol.6, No.4, (2012).

14. Magnesium Elektron 21 Datasheet 455, www.magnesium-elektron.com

15. Magnesium Elektron WE43B Datasheet 467A & Datasheet 478, www.magnesium-elektron.com.